ELSEVIER

Applied Surface Science 197–198 (2002) 130–137

applied surface science

www.elsevier.com/locate/apsusc

# Atmospheric pressure matrix-assisted laser desorption ionization as a plume diagnostic tool in laser evaporation methods

John H. Callahan[a], Marsha C. Galicia[b], Akos Vertes[b,*]

[a]*Naval Research Laboratory, Chemical Dynamics and Diagnostics Branch, Code 6110, Washington, DC 20375, USA*
[b]*Department of Chemistry, George Washington University, Washington, DC 20052, USA*

**Abstract**

Laser evaporation techniques, including matrix-assisted pulsed laser evaporation (MAPLE), are attracting increasing attention due to their ability to deposit thin layers of undegraded synthetic and biopolymers. Laser evaporation methods can be implemented in reflection geometry with the laser and the substrate positioned on the same side of the target. In some applications (e.g. direct write, DW), however, transmission geometry is used, i.e. the thin target is placed between the laser and the substrate. In this case, the laser pulse perforates the target and transfers some target material to the substrate. In order to optimize evaporation processes it is important to know the composition of the target plume and the material deposited from the plume. We used a recently introduced analytical method, atmospheric pressure matrix-assisted laser desorption ionization (AP-MALDI) to characterize the ionic components of the plume both in reflection and in transmission geometry. This technique can also be used to directly probe materials deposited on surfaces (such as glass slides) by laser evaporation methods. The test compound (small peptides, e.g. Angiotensin I, ATI or Substance P) was mixed with a MALDI matrix (α-cyano-4-hydroxycinnamic acid (CHCA), sinapinic acid (SA) or 2,5-dihydroxybenzoic acid (DHB)) and applied to the stainless steel (reflection geometry) or transparent conducting (transmission geometry) target holder. In addition to the classical dried droplet method, we also used electrospray target deposition to gain better control of crystallite size, thickness and homogeneity. The target was mounted in front of the inlet orifice of an ion trap mass spectrometer (IT-MS) that sampled the ionic components of the plume generated by a nitrogen laser. We studied the effect of several parameters, such as, the orifice to target distance, illumination geometry, extracting voltage distribution and sample preparation on the generated ions. Various analyte–matrix and matrix–matrix cluster ions were observed with relatively low abundance of the matrix ions.


*Keywords:* MAPLE; Direct write; Atmospheric pressure MALDI; Laser evaporation; Plume diagnostics

## 1. Introduction

Diagnostics of the transient plume induced in pulsed laser deposition (PLD) experiments is essential for the production of thin solid films [1] and nanoscopic materials [2] with desired characteristics. Expansion dynamics has been followed by imaging of the plume with gated, intensified CCD [3]. The chemical composition of the plume has also been probed with mass spectrometric (MS) methods [4,5].

Recently, a new method, matrix-assisted pulsed laser evaporation (MAPLE), has emerged for the deposition of organic, polymeric and biological thin films [6–9]. It has been shown that MAPLE is capable of producing biopolymer layers that retain their biological

* Corresponding author. Tel.: +1-202-994-2717; fax: +1-202-994-5873.
*E-mail address:* vertes@gwu.edu (A. Vertes).

0169-4332/02/$ – see front matter 
PII: S0169-4332(02)00316-1

activity [9]. Characterization of the MAPLE plume is essential to deliver on the promise of thin organic layers with predictable and reproducible properties [10]. Although imaging studies [11,12] and MS investigations [13,14] have been reported for plumes typical in matrix-assisted laser desorption ionization (MALDI), the conditions, primarily the pressure, in MAPLE are significantly different. While the typical pressure in a MALDI experiment is $\sim 10^{-6}$ Torr, the external pressure in MAPLE can be anywhere between $5 \times 10^{-2}$ Torr and atmospheric pressure (AP) [15]. In MALDI, forward-peaked plume density distributions were observed for the both matrix and the guest species [12,13] with significantly narrower angular distribution for the guests (plume sharpening effect) [12]. Plume sharpening, if it also exists at elevated pressures, has very significant implications for the delivery of guest species in MAPLE applications.

Laser induced forward transfer (LIFT) and direct write (DW) technologies in combination with MAPLE promise the maskless production of electronic components and sensors on a microscopic scale [15–18]. In the DW-MAPLE process, the matrix containing the material to be transferred is deposited on a transparent substrate. The back illumination of the target through substrate and resultant laser ablation of the material results in the transfer of the material of interest onto an acceptor substrate. Distinct advantages of these methods include rapid prototyping of new patterns and sensing surfaces at room temperature and at AP. Using this technology, active and passive circuit elements have been produced with better than 10 μm resolution.

Ultrahigh speed optical microscopy was used to follow plume expansion in DW-MAPLE [19]. Following the plume expansion generated by a 150 ns frequency tripled Nd: YAG laser pulse from barium–zirconium titanate embedded in α-terpineol matrix showed that material removal does not start until 200 ns and continues for up to 1 μs. The plume consisted of evaporated matrix as well as particulate matter.

Gas dynamic description of the laser induced plasma showed a significant slowdown of the plume expansion in the presence of a background gas [20]. Using this approach, the film thickness profile and the apparent rotation of the plume can also be explained [21]. Molecular dynamics modeling of the MAPLE process indicates the presence of two regimes: stress confinement for laser pulse lengths shorter than the stress propagation time and thermal confinement for longer pulses [22].

Due to the presence of ambient gas, plume composition measurements are not available for MAPLE and DW-MAPLE. A recently discovered analytical method, AP-MALDI, utilizing orthogonal extraction time-of-flight MS is capable of sampling laser-induced plumes at elevated pressures [23,24]. Further studies have shown that similar results can be achieved using ion trap (IT) mass analyzers [25–27]. These results, however, were obtained in reflection geometry, i.e. with the laser illumination and ion extraction arranged on the same side of the sample. While MAPLE relies on reflection geometry, in the DW technology, transmission geometry is utilized, i.e. laser illumination and plume formation are on the opposite sides of the target. Transmission geometry MALDI was successfully introduced in vacuum environment [28]. Recently, transmission geometry AP-MALDI has also been demonstrated as an analytical method [29].

In the present communication, we report on the application of transmission geometry AP-MALDI for the characterization of the ionic components in DW-MAPLE plumes. Comparison with our earlier results on the use of AP-MALDI for the diagnostics of MAPLE plumes is made. We are also interested to see if plume sharpening effects exist under conditions similar to DW-MAPLE. Potential use of the transmission geometry AP-MALDI in the analysis of thin films deposited by MAPLE is explored.

## 2. Experimental

### 2.1. Instrument

The reflection and transmission geometry MAPLE systems for plume analysis consisted of home-built sample stages, a nitrogen laser (VSL-337ND, Laser Science Inc., Franklin, MA) and a Finnigan LCQ ion trap mass spectrometer, IT-MS (Finnigan MAT, San Jose, CA). The experimental arrangement for reflection and transmission geometries with the two variants of the sample stage is shown in Fig. 1a and b, respectively. The ion source region of the Finnigan

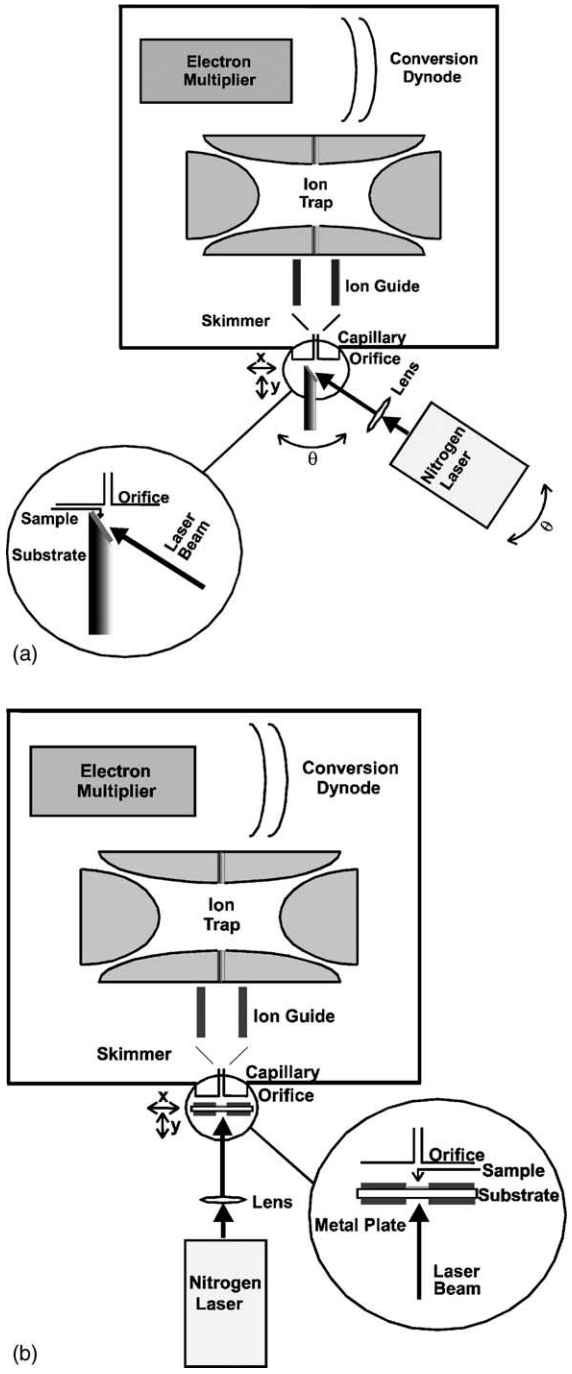


Fig. 1. AP-MALDI with IT detection for plume characterization in MAPLE and DW-MAPLE using: (a) reflection and (b) transmission geometry. Sample illumination is shown in the insets.

LCQ IT-MS was replaced with the home-built AP-MALDI component. The nitrogen laser provided ultraviolet radiation (337 nm) for the experiments with a laser fluence of approximately 0.07 J/cm$^2$ per pulse in the focal spot of the 20 cm focal length biconvex lens.

Several target geometries were evaluated including a flat top, flat top with a repeller piece, an angled top and various transparent sandwich structures. For reflection geometry, the highest ion yield was observed using a stainless steel cylindrical target with a surface angled at about 45°. This target was used for most of the reflection geometry studies. In transmission geometry, different types of transparent slides served as sample substrates, i.e. a quartz slide with transparent indium–tin oxide (ITO; ITO coated polished fused quartz slide, Delta Technologies, Ltd., Stillwater, MN) conductive coating, a glass microscope slide, and a silanized glass microscope slide. The silanized glass microscope slide was prepared using a method described in the literature [30]. The slide was sandwiched between two metal plates with center holes in order to apply the high voltage and be able to illuminate the sample (see inset of Fig. 1b). A micropositioning stage allowed for translation of the target in the *x*-, *y*-, and *z*-directions with 0.1 mm accuracy. The illuminated portion of the target was set approximately 2–5 mm from the 0.51 mm diameter orifice. The applied sample voltage was varied between 0 and 3.0 kV. In both geometries, a voltage of ∼2.0 kV was determined to provide the best ion collection efficiency into the IT orifice.

For single laser shots per scan, the IT injection time was set to 400 ms, while the laser shot was triggered 300 ms after the scan start by a delay generator (DG535, Stanford Research Systems, Sunnyvale, CA). Higher sensitivity could be achieved in burst mode (multiple laser shots per scan) utilizing a waveform generator (Model 39 Universal Waveform Generator, Wavetek, Ltd., Norwich, Norfolk, UK) and the delay generator. In this arrangement, a longer injection time was necessary, therefore, the injection time was extended to 800 and 1200 ms. The laser trigger delay times were adjusted to 410 and 610 ms, respectively. The laser bursts begin at the time of laser trigger for a period of 400 ms (for 800 ms injection time) or 600 ms (for 1200 ms injection time) at a frequency

of 20 Hz. The IT for the full scan MS mode was set to standard operating parameters obtained from optimal instrument tuning. The ion injection time was varied between 200 and 1200 ms. Optimum signal intensity was achieved with the tube lens offset and capillary voltage set to 0 V and the capillary temperature to 190 °C.

For conventional MALDI, a home-built MALDI-TOF instrument was used [31].

### 2.2. Sample preparation

The matrix compounds used were α-cyano-4-hydroxycinnamic acid (CHCA), sinapinic acid (SA), 2,5-dihydroxybenzoic acid (DHB), and 2-(4-hydroxyphenylazo)-benzoic acid (HABA), were all purchased from Aldrich Chemical Co. (Milwaukee, WI). They were used without purification. The matrices, except HABA, were prepared as saturated solutions in 70% (v/v) HPLC grade acetonitrile (Fisher Scientific Company, Fair Lawn, NJ) prepared in deionized water (18.2 MΩ/cm). The HABA was prepared in anhydrous methanol (Mallinckrodt Baker, Inc., Paris, KY). The solute compounds (Angiotensin I (ATI), Substance P, Leucine Enkephalin, Insulin, Met-Arg-Phe-Ala (MRFA), Lys-Trp-Lys (KWK), L-α-Phosphatidylcholine, Cytochrome C, Trypsin and polyethylene glycol 600 and 1450 (PEG 600, PEG 1450)) were supplied by Sigma. The biological materials and the CHCA matrix were stored in the freezer. Solutions of the biological materials were prepared in deionized water (18.2 MΩ/cm; or, if necessary, 0.1% trifluoroacetic acid in water) between concentrations 1 and $4 \times 10^{-4}$ M. The polymers were dissolved in anhydrous methanol (Mallinckrodt Baker, Inc., Paris, KY) at concentrations between $7 \times 10^{-4}$ and $5 \times 10^{-3}$ M. Using a procedure described previously, intact insulin was reduced into its two building units, Chain A and Chain B [32].

To prepare samples for laser evaporation, a 1 or 2 μl aliquot of a 1:5 (v/v) solute–matrix mixture was deposited on the target and allowed to air dry in 3–5 min (dried droplet method). In some cases, the two-layer method or electrospray sample deposition was also used [33]. Electrospray deposition at 3.5–5.0 kV capillary voltages and 2.5 μl/min flow rate onto a substrate placed 3.0 cm from the tip resulted in a uniform target of 1–3 μm thickness in 0.5–1.5 min.

## 3. Results and discussion

MS has extensively been used in plume diagnostics in a vacuum environment. The first question we wanted to answer was whether MS could be utilized in the characterization of MAPLE and DW-MAPLE type plumes at APs. To test feasibility, biopolymer samples were prepared in CHCA matrix using the dried droplet or the electrospray method. A cylindrical angled top stainless steel target was used for reflection geometry. Initially, a quartz slide with transparent ITO coating was used as a target in transmission geometry. Quartz was selected to minimize the attenuation of the laser intensity and the conductive ITO coating was expected to improve ion collection efficiency by providing a homogeneous field in the plume region. In subsequent experiments, a glass microscope slide was used as both of these provisions turned out to be unnecessary.

Mass spectra of Substance P/CHCA plume in reflection geometry and ATI/CHCA plume in transmission geometry are shown in Fig. 2 as examples. The Substance P spectrum (Fig. 2a) shows the protonated molecular ion of the Substance P ($m/z$ 1347.8) and an adduct ion with two CHCA molecules attached ($m/z$ 1724.8). Remarkably, there are no matrix ions or matrix fragments detected in the spectrum. In transmission geometry, the spectrum is even simpler. Fig. 2b shows the protonated molecular ion ($m/z$ 1296.5) as the only significant ionic component in the ATI/CHCA plume.

There are several important differences between the mass spectra taken at AP and in vacuum. The formation of matrix adducts derived from the biopolymer ion is well known in vacuum MALDI at ultraviolet wavelengths. Typically, the adduction of only one matrix molecule is observed. The occasional adduction of subsequent matrix molecules results in increasingly reduced adduct ion abundances [34]. It is also known that CHCA has a weak tendency to form matrix cluster ions [35]. Based on these observations it comes as a surprise that strong matrix adduct peaks are observed in the reflection mode AP-MALDI spectra. Even more surprising is the fact that under certain conditions primarily the adduction of even number of matrix molecules is observed in these experiments (see Fig. 2a and [24]).

This latter effect is probably related to the predominance of carboxyl-bound dimers in organic acids in

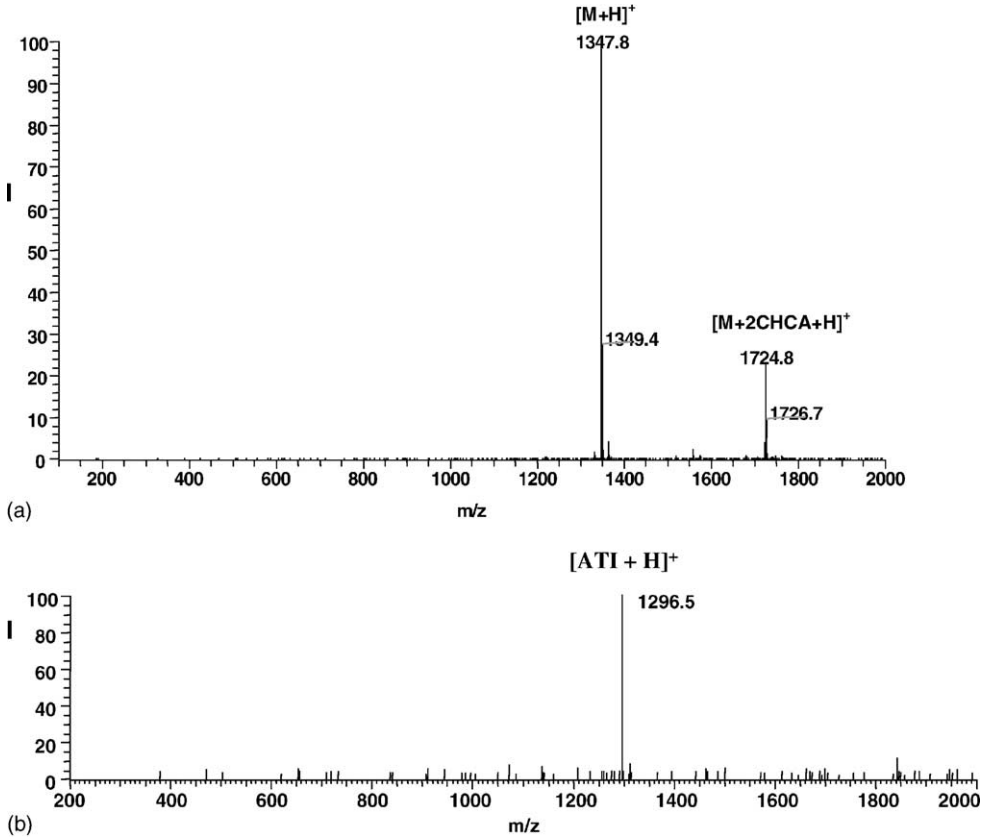


Fig. 2. Ionic plume components recorded by IT-MS. Substance P evaporated from CHCA matrix in reflection geometry (a) and ATI evaporated from CHCA in transmission geometry (b).

the condensed phase. Organic acids (like the matrices in this study) are known to form dimers in solid and liquid phase. The carboxyl groups pair up with the –C(OH)=O pointing to the H–O–CO– to form –C(OH)=O. . .HO–CO– and vice versa. The resulting structure is a ring with two hydrogen bonds. In the reflection geometry AP-MALDI spectra of the YGGFL peptide, matrix dimer and tetramer ions are abundant (see Fig. 3a). We have also seen dimerization in the molecular modeling of SA crystals (see Fig. 3b) [37]. At the same time, there is no molecular ion or trimer for the matrix in the spectra. This observation supports the idea that the matrix dimers indeed originate from the solid phase, survive the volatilization and enter the plume. Since dimers are the predominant matrix species in the plume, the formation of the corresponding biopolymer adduct ions is also preferred. There is another question remaining: how does such a dimer attach to a peptide ion? According to a recent study, matrix adduct formation is facilitated by Arg residues [27] in AP-MALDI. As the side chain of Arg is basic and the matrix is acidic, this suggests acid base chemistry. Perhaps partial opening of the quasi-ring formed from the two acidic carboxyl groups leads to interaction with the basic Arg side chain.

This is further supported by the observation that upon collisional activation in the IT, both matrix molecules fall off the peptide at the same collision energy. That is, the dimer is not bound in such a way that one matrix molecule falls off, then the other. This argues for a structure in which the dimer maintains its structure to some degree when it is bound to the peptide. Perhaps the ring formed by the carboxylate groups is centered over the charge site so that the various oxygen atoms (carbonyl and carboxylic acid) interact with the charge. Such a structure would be most likely observed where

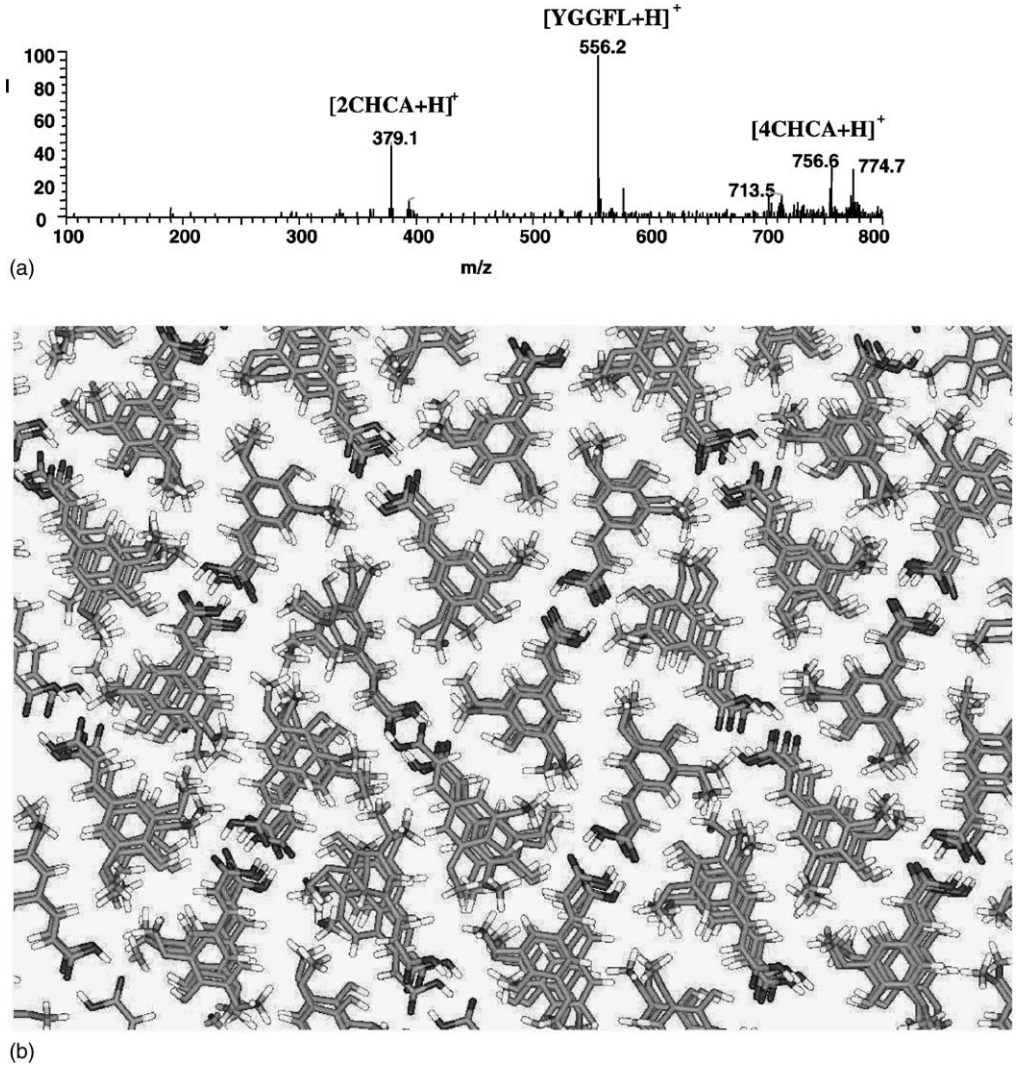


Fig. 3. (a) Dimer (*m*/*z* 379.1) and tetramer (*m*/*z* 756.6) species of CHCA matrix are observed in reflection geometry plumes during the evaporation of YGGFL peptide. (b) Similar dimerization of SA is observed in computational modeling of solid matrix [37]. Two matrix molecules are held together by two hydrogen bonds between the carboxyl groups.

the charge, in this case a proton, is accessible on a side chain of the peptide, as is the case with Arg.

A possible explanation of the enhanced adduct formation under AP conditions can be based on the effect of ambient gas on the expanding plume. The slowdown of plume expansion [20] and the thermalization of ions through multiple collisions with the background gas both favor a transition from kinetic control in the plume to thermodynamic control. In other words, there is more time for the plume components to react (due to the slowdown) and the reactants are less energetic thus approaching thermodynamic equilibrium in their properties. The abundance of cluster ions increases with the increasing the molecular weight of the biopolymer [24] and with the introduction of arginine residues [27]. As the most basic residue in MALDI [31], arginine may promote acid–base chemistry between the peptide and the acidic matrix molecules.

From the analytical perspective matrix adduct formation is a nuisance as it decreases sensitivity and

leads to more complex spectra. From the point of view of MAPLE and DW-MAPLE these adducts can also present a problem if they incorporate into the deposited layer and alter its properties. Although this observation is preliminary in nature, there is an interesting difference when reflection and transmission geometry AP-MALDI spectra are compared (see Fig. 2a and b, respectively). Transmission geometry plumes do not seem to exhibit matrix adduct formation. If this observation is confirmed by further experiments, it has a major significance both for the MAPLE-type preparative and for the analytical applications.

An important difference between vacuum MALDI and AP laser evaporation plumes is the relatively low abundance [27] or even the complete lack of matrix and matrix fragment ions (see Fig. 2a) in the latter. There are several potential explanations for this phenomenon. It is known from vacuum MALDI studies that reduced matrix to biomolecule molar ratios can lead to the elimination of matrix ions from the spectra [36]. This, so called, matrix suppression effect, however, requires elevated biopolymer concentrations in the solid phase, a condition not present in our experiments.

Another potential explanation for the lack of matrix ions is based on the dynamics of plume expansion. Imaging studies of the MALDI plume showed that the matrix molecules had comparable radial and axial velocities, whereas the heavier biomolecules had a higher axial velocity component, leading to plume sharpening [12]. For dye-tagged DNAase I biopolymer (30,000 Da) and 3-hydroxypicolinic acid (3-HPA, 139 Da) matrix it was shown that the matrix plume reaches a 2:1 ratio in its axial to radial front velocities in $\sim$10 μs, whereas the biopolymer plume expands with an 8:1 anisotropy established in $\sim$50 μs. This difference in angular distribution leads to significant separation of the two plumes that can contribute to the selective detection of the heavy component. Since the acceptance ratio (orifice to target distance/orifice radius) is $\sim$12:1 in our experiment, it is possible that the heavier plume components are collected preferentially. For lighter biopolymers, however, the plume sharpening effect is expected to diminish.

In addition, under atmospheric conditions, the presence of the background gas results in collisional slowdown of the plume. Because the matrix ions have lower molecular weight than the biomolecules, they undergo isotropic scattering, whereas the higher molecular weight biopolymer ions exhibit significant forward scattering. Thus, the large ions are favored to reach the MS orifice.

Finally, we also need to consider an instrumental artifact as a potential explanation. When detecting the relatively high mass biopolymer ions, the IT might discriminate against the low molecular weight matrix ions. This argument, however, is not very strong. Even when analyzing the CHCA matrix plume in low mass mode with no biomolecules present, the matrix ion intensity was relatively low. The matrix/analyte signal intensity ratio in conventional MALDI is often very large. Even if one assumes it is only 10:1, nearly 1:1000 mass discrimination effect (1 matrix ion detected for 1000 analyte ions) would be needed to explain the absence of matrix peaks in the AP-MALDI spectra. Mass bias of this magnitude is unlikely, as it would relegate the IT useless in analytical applications.

## 4. Conclusions

In this study, we demonstrated that AP-MALDI could be used as a plume diagnostic tool both in reflection (MAPLE) and in transmission geometry (DW-MAPLE). This method provides direct information on the nature and abundance of ionic plume components. AP-MALDI exhibits excellent sensitivity and good dynamic range enabling the detection of trace as well as major components in the plume.

Evidence was found for plume fractionation under atmospheric conditions. In particular, preferential forward transport of heavy components was observed. This is specifically important for the DW-MAPLE of mixtures, as the film composition can be significantly different from the composition of the target. Learning the relationship between the composition of the target, the plume and the deposited film facilitates finding targets that result in films with the desired constituents. Transition geometry AP-MALDI is also a good candidate for the analysis of films deposited on transparent substrates.

Clustering of the matrix species and between the matrix and biopolymer molecules was uncovered. In the biopolymer/CHCA plume, we detected the preferential adduction of matrix dimers and tetramers to

biopolymer ions. This phenomenon could be attributed to the presence of preformed matrix dimers in the solid phase. Clearly, the chemistry between the matrix and biopolymer species in the plume plays a major role in determining the properties of the deposited film. In summary, we demonstrated that AP-MALDI is well positioned to detect chemical changes in MAPLE and DW-MAPLE plumes.

## Acknowledgements

This work was supported by the Office of Naval Research on contract #N00014-00-WX20319. One of the authors, M.C.G., is grateful for the financial assistance by the Naval Research Laboratory via Geo-Centers Inc. Part of this research was supported by a grant from the National Science Foundation (CHE-9873610) and from the Department of Energy (DE-FG02-01ER15129).

## References

[1] D.H. Lowndes, D.B. Geohegan, A.A. Puretzky, D.P. Norton, C.M. Rouleau, Science 273 (1996) 898.
[2] A.A. Puretzky, D.B. Geohegan, X. Fan, S.J. Pennycook, Appl. Phys. A: Mater. Sci. Process 70 (2000) 153.
[3] D.B. Geohegan, Appl. Phys. Lett. 60 (1992) 2732.
[4] R. Zheng, M. Campbell, K.W.D. Ledingham, W. Jia, C.T.J. Scott, R.P. Singhal, Spectrochim. Acta B 52 (1997) 339.
[5] T. Mathews, J.R. Sellar, B.C. Muddle, P. Manoravi, Chem. Mater. 12 (2000) 917.
[6] R.A. McGill, R. Chung, D.B. Chrisey, P.C. Dorsey, P. Matthews, A. Pique, T.E. Mlsna, J.I. Stepnowski, IEEE Trans. Ultrason. Ferroelectr. Freq. Contr. 45 (1998) 1370.
[7] A. Pique, R.A. McGill, D.B. Chrisey, D. Leonhardt, T.E. Mslna, B.J. Spargo, J.H. Callahan, R.W. Vachet, R. Chung, M.A. Bucaro, Thin Solid Films 356 (1999) 536.
[8] D.M. Bubb, B.R. Ringeisen, J.H. Callahan, M. Galicia, A. Vertes, J.S. Horwitz, R.A. McGill, E.J. Houser, P.K. Wu, A. Pique, D.B. Chrisey, Appl. Phys. A: Mater. Sci. Process 73 (2001) 121.
[9] B.R. Ringeisen, J.H. Callahan, P.K. Wu, A. Pique, B. Spargo, R.A. McGill, M. Bucaro, H. Kim, D.M. Bubb, D.B. Chrisey, Langmuir 17 (2001) 3472.
[10] D. Young, H.D. Wu, R.C.Y. Auyeung, R. Modi, J. Fitz-Gerald, A. Pique, D.B. Chrisey, P. Atanassova, T. Kodas, J. Mater. Res. 16 (2001) 1720.
[11] A.A. Puretzky, D.B. Geohegan, Chem. Phys. Lett. 286 (1998) 425.
[12] A.A. Puretzky, D.B. Geohegan, G.B. Hurst, M.V. Buchanan, B.S. Luk'yanchuk, Phys. Rev. Lett. 83 (1999) 444.
[13] B. Spengler, V. Bokelmann, Nucl. Instrum. Meth. B 82 (1993) 379.
[14] G.R. Kinsel, M.E. Gimon-Kinsel, K.J. Gillig, D.H. Russell, J. Mass Spectrom. 34 (1999) 684.
[15] D.B. Chrisey, A. Pique, J. Fitz-Gerald, R.C.Y. Auyeung, R.A. Mcgill, H.D. Wu, M. Duignan, Appl. Surf. Sci. 154 (2000) 593.
[16] A. Pique, D.B. Chrisey, R.C.Y. Auyeung, J. Fitz-Gerald, H.D. Wu, R.A. McGill, S. Lakeou, P.K. Wu, V. Nguyen, M. Duignan, Appl. Phys. A—Mater. Sci. Process 69 (1999) S279Suppl. S.
[17] A. Pique, D.B. Chrisey, J.M. Fitz-Gerald, R.A. Mcgill, R.C.Y. Auyeung, W.J. Wu, S. Lakeou, V. Nguyen, R. Chung, M. Duignan, J. Mater. Res. 15 (2000) 1872.
[18] D.B. Chrisey, A. Pique, R. Modi, H.D. Wu, R.C.Y. Auyeung, H.D. Young, Appl. Surf. Sci. 168 (2000) 345.
[19] D. Young, R.C.Y. Auyeung, A. Pique, D.B. Chrisey, D.D. Dlott, Appl. Phys. Lett. 78 (2001) 3169.
[20] A. Vertes, in: J.C. Miller, D.B. Geohegan (Eds.), Laser Ablation: Mechanisms and Applications II, AIP Press, New York, 1994, p. 275.
[21] S.I. Anisimov, B.S. Lukyanchuk, A. Luches, Appl. Surf. Sci. 96 (8) (1996) 24.
[22] T.E. Itina, L.V. Zhigilei, B.J. Garrison, Nucl. Instrum. Meth. B 180 (2001) 238.
[23] V.V. Laiko, A.L. Burlingame, US Patent 5,965,884 (1999).
[24] V.V. Laiko, M.A. Baldwin, A.L. Burlingame, Anal. Chem. 72 (2000) 652.
[25] J.H. Callahan, M. Galicia, A. Vertes, in: Proceedings of the 48th ASMS Conference on Mass Spectrometry and Allied Topics, Long Beach, CA, 11–15 June 2000.
[26] R.A. Danell, G.L. Glish, in: Proceedings of the 48th ASMS Conference on Mass Spectrometry and Allied Topics, Long Beach, CA, 11–15 June 2000.
[27] V.V. Laiko, S.C. Moyer, R.J. Cotter, Anal. Chem. 72 (2000) 5239.
[28] A. Vertes, L. Balazs, R. Gijbels, Rapid Commun. Mass Spectrom. 4 (1990) 263.
[29] M.C. Galicia, A. Vertes, J.H. Callahan, Anal. Chem. 74 (2002) 1891.
[30] D. A Stenger, J.H. Georger, C.S. Dulcey, J.J. Hickman, A.S. Rudolph, T.B. Nielsen, S.M. McCort, J.M. Calvert, J. Am. Chem. Soc. 114 (1992) 8435.
[31] Z. Olumee, M. Sadeghi, X. Tang, A. Vertes, Rapid Commun. Mass Spectrom. 9 (1995) 744.
[32] X. Tang, R. Donaldson, A. Vertes, in: Proceedings of the 41st ASMS Conference on Mass Spectrometry and Allied Topics, San Francisco, CA, 31 May–4 June 1993, p. 666.
[33] Y.Q. Dai, R.M. Whittal, L. Li, Anal. Chem. 68 (1996) 2494.
[34] W. Zhang, S. Niu, B.T. Chait, J. Am. Soc. Mass Spectrom. 9 (1998) 879.
[35] B.O. Keller, L. Li, J. Am. Soc. Mass Spectrom. 11 (2000) 88.
[36] R. Knochenmuss, F. Dubois, M.J. Dale, R. Zenobi, Rapid Commun. Mass Spectrom. 10 (1996) 871.
[37] M. Sadeghi, X. Wu, A. Vertes, J. Phys. Chem. B 105 (2001) 2578.